Chapter 2

SELF-ORGANIZED MICROLENS FABRICATION AND HIGH-RESOLUTION IMAGING IN A MICROFLUIDIC CHANNEL

2.1 CHAPTER OUTLINE

In this chapter, we have demonstrated the fabrication of a polymer micro-lens array by self-organized dewetting inside the microchannel, which shows remarkable enhancement in the resolution, contrast, and more than 10 times add-on magnification to a microscope. These lenses are demonstrated to resolve sub-micrometer features and detect moving micro-particles when the suspension is flown in a microchannel. Polystyrene (PS) micro-lenses are fabricated on a polydimethylsiloxane (PDMS) substrate using the controlled dewetting of PS thin film then this PDMS substrate is used to close the microchannel with inverted micro-lenses. An aqueous suspension of polystyrene beads is flown through the microchannel and we observed the particles through an optical microscope. Focusing and magnification through PS micro-lenses are analyzed to get a quantitative estimate of the particle number density in the solution. This method offers a promising low-cost high throughput solution for determining the approximate number density of flowing particles or suitably stained biological cells. Particularly in a pathology lab, it can tremendously increase detection limits by enabling the visibility of sub-micrometer pathogens using a standard laboratory microscope.

2.2 INTRODUCTION

Miniaturized lenses, their arrays, and integrated imaging systems are of great interest in recent years because of their excellent light collection efficiencies. Micro-lenses have

been successfully demonstrated to be used in 3D lithography,[1] photolithography,[2] optical interconnectors,[3] optical communication systems,[4] integral imaging, and 3D display,[5] OLEDs, and integrated optics components.[6,7] With the progress in optofluidics and electronics, miniature lenses have shown great and ever-increasing importance in sensing and detection.[8-10] Micro-lenses have been studied for a wide range of applications from focusing on high energy X-Rays,[11] diffusers[12] to the analysis of microarrays of DNA.[13] In the past several years, different methods including droplet casting[14] and hot embossing[15] have been explored for the fabrication of micro-lenses which work well for lenses of a few micrometers in size or larger but smaller lenses suffer from irregularities and defects. However, a recently reported technique to fabricate nearly defect-free spherical microlenses using self-organized dewetting[16] and crystallization[17] has demonstrated the use of nano-lenses for sub-diffraction limit imaging.

Microlens arrays have been used to increase the luminous power efficiencies in OLEDs,[7] used as homogenizers for excimer laser,[18] and in the collimation of light in the microchip.[19] Microlenses have also been used as biomimetic optical elements which can be used similarly to a compound eye system of insects.[20] These compound eye systems of microlenses provide high depth of field, low aberration and distortion, extremely large field of view, and fast temporal resolution, compared to single aperture eyes.[20,21] This is due to the short focal length of each microlens and the nature of image formation. However, the compound eye system has an inherent drawback of low spatial resolution. A compound eye imaging module has been used in fingerprint capturing.[22] Various techniques for the fabrication of compound eye microlens systems have been proposed via the surface wrinkling method,[23] lithography, micromachining, and imprinting processes.[24]

2.2.1 Microlens fabrication

The first important aspect of the making of the microlens is the method of fabrication. There are several methods investigated to fabricate the microlens and their arrays. Some of the most important fabrication methods are by using direct laser printing,[25] thermally curing photosensitive gel film,[26] thermal reflows of ultrathin nanofilm,[27] enhanced dewetting of polymer film,[16] electrically templated dewetting of a UV curable polymer film,[28] using femtosecond laser pulses to fabricate concave microlens array.[29] Most of the above-mentioned fabrication techniques are top-down, resource intensive, and slow as they rely on serial micromachining. These processes are slow, use sophisticated machines and materials which make them expensive, are limited in spatial resolution, and have a low optical quality finish. One technique that stands out here is self-organized dewetting[16,28] which provides benefits from both top-down and bottom-up fabrication methods. One can easily control the size and spacing between lenses by controlling the initial film thickness whereas the interfacial tension takes care of an optically smooth surface finish.[30-33] Being a spontaneous fabrication method, it is inexpensive and the use of common thermoplastic polymers makes it a versatile technique.

2.2.2 Material Selection

The second equally important aspect of lens fabrication is material selection. Materials used for lens fabrication are primarily polymeric materials. Self-assembling, reflow properties, and high optical transmittance of polymers offer easy tailoring of optical structures. The shape of polymer microlens can be tuned using thermal, electric, magnetic, or pH stimulation.[34] However, due to the lower refractive index than glass and low stability under solvent and thermal treatment, some polymer microlenses can be limited in their use. Therefore, we have selected polystyrene which has a higher refractive

index (n =1.59), is thermally stable up to 100°C (T_g >100°C), and is resistant to most of the aqueous solutions.[35]

2.2.3 Application of Microlens Arrays

The next important aspect is the application of microlens and arrays in high-resolution imaging. In most of the earlier reported imaging techniques, microlenses have been used to focus on a stationary micro-pattern such as lithographically patterned substrates and immobilized biological cells and organisms, and enhancement in magnification and improvement in resolution from an individual lens has been reported.[16,17,36] However, for moving objects such as suspended particles flowing in a microfluidic channel, the use of an individual lens for enhanced magnification and their positioning is still a challenge. In this chapter, we have demonstrated a simple method of fabrication of polymeric microlenses of polystyrene of 1-100 μm size on flexible PDMS substrate using intensified dewetting of polymer thin film.[37] These polymeric lenses have shown up to 10 times enhancement in magnification and improved spatial resolution when used together with 20X/(NA 0.40) and 10X/(NA 0.25) objectives of a microscope. These lenses can form upright as well as inverted images, depending on the working distance, and provide a high depth of focus with a reasonable depth of field. By incorporating these micro-lenses in the microchannel we have demonstrated that these can focus on moving particles in the proximity of the focal point of the lenses. These lenses can significantly increase the magnification and contrast of the image by collecting more diffracted light from the object in a microchannel. This technique has the potential to be used in the estimation of the number of biological cells, tissues, micro-organisms, and other selectively tagged analytes present in culture by flowing in the microchannel. This method enables the use of microlenses in conjunction with a typical optical microscope to obtain more than 10 times add-on magnification without any significant investment.

2.3 EXPERIMENTAL METHODS

The experimental method consisted of different segments such as lens fabrication, the microfluidic embedding of lenses, imaging of flowing particles, and image processing and number estimation. Details of the different approaches are given below.

2.3.1 Polystyrene Lens Fabrication

Polystyrene (PS) solution in toluene, of different concentrations, was spin-coated over a thoroughly cleaned glass substrate. Afterward, the film was floated on water and then captured over a flat PDMS substrate.[33] To float the thin film from the glass slide, the corner of the thin film was scratched to remove the pinning effect of the film on the glass slide. Holding the slide along with the film was dipped in the DI water Petri dish. A crosslinked PDMS substrate of 15mm×15mm was taken below the floated film in the water and lifted to carry up the film on the PDMS substrate. Floating the film from the glass slide to PDMS releases the residual stress in the thin film. Directly coating the PS on the PDMS film takes a too long time to dewett, and is difficult to get the spherical droplets even after equilibrium is achieved. Intensified dewetting of PS film is done in a mixture of water, methyl ethyl ketone, and acetone in a ratio of 10:7:3.[16,38] After complete dewetting, samples were dried in air and then heated for four hours at 180° C in a vacuum oven to remove any entrapped liquid in the polymer.

2.3.2 Development of a Microfluidic Chip Platform for Particle Observation

To fabricate a straight microchannel in PDMS, Sylgard 184 (Dow corning) with 10% crosslinker was pored over a stainless steel wire of 100 μm diameter and cured in an oven at 120° C for four hours to complete the crosslinking reaction. Afterward, the substrate

was soaked in acetone to slightly swell PDMS and stainless steel wire was pulled out from the microchannel with 100µm depth.

In the next step, the lenses fabricated were inverted into the microchannel. To incorporate microlenses into the microchannel, the PDMS substrate with dewetted PS droplets described in section 2.3.1, was inverted and bonded with the channel-carved PDMS substrate mentioned in the previous paragraph. Thus a closed microchannel with a flat top surface with dewetted pattern hanging inside the channel was obtained as shown in the schematic diagram in figure 2.1. Bonding of the two substrates was done by manually coating a thin layer of PDMS over the channel-carved substrate, and heating it at 120°C for two hours after inverting the dewetted lenses over it. While inversion of PDMS substrate containing microlenses, due care should be taken if it slides over the substrate containing channel. PDMS used for bonding may slip in between lenses and channels, if two substrates slide over each other.

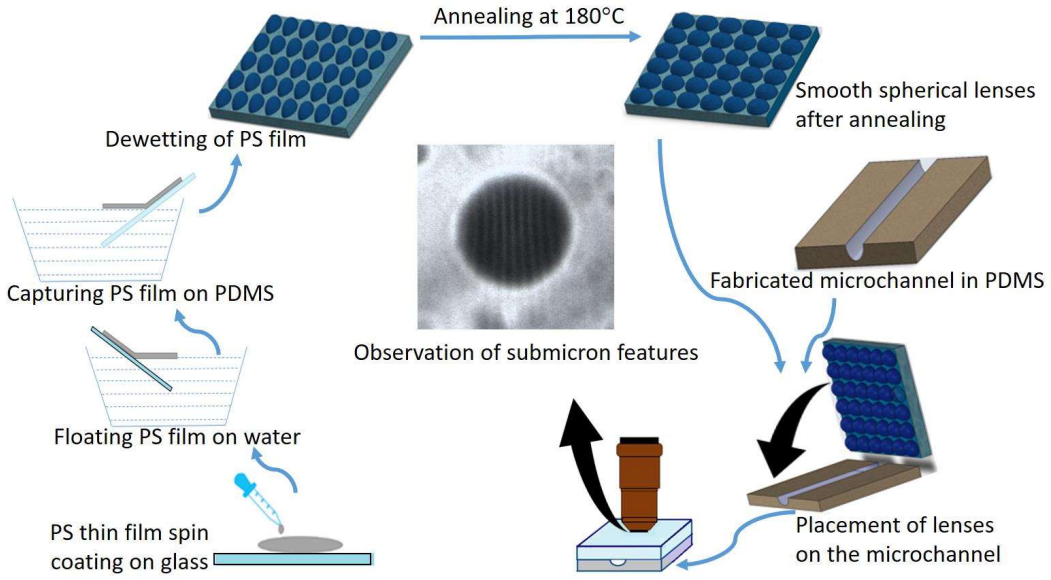

Figure 2.1 Schematic diagram of the fabrication of polymer lens array and its embedding in the microchannel.

To analyze focusing through micro-lenses, various micropatterns were observed using an optical microscope, and magnification with and without microlenses was compared. Moreover, polystyrene microparticles (3.0μm) from Thermofisher Scientific were injected into the fabricated microchannel using a syringe pump. The flowing particles were observed using an optical microscope at different magnifications with and without microlenses.

2.3.3 Image Processing

The images of microparticles were analyzed using ImageJ software to count the number of particles in a snapshot and this information is used further in the estimation of particle number density in the flowing media. A selected section of lenses depicting particles is cropped for the counting interest. The cropped image is converted from RGB to an 8-bit image and subjected to thresholding, water-shedding, and brightness and contrast adjustments manually. Image J application provides the necessary information like no. of particles their size, perimeter, sphericity, etc.

2.4 RESULT AND DISCUSSION

Firstly the quality of lenses and their effectiveness in the observation of still pattern was demonstrated, then moving particle was observed. Afterward, imaging, particle observations, and their number estimation were done. Detailed results are as follows-

2.4.1 Fabricated lens and Their Quality

Polystyrene has a higher refractive index than optical glass and quartz which are by far the most commonly used materials in optical elements. In addition, it also has fairly high transmittance for visible light. The major component in the cost of miniature optical components arises from the fabrication cost which includes micro-machining, and

precision grinding for defect-free optically smooth finishing. To overcome this we relied on the interfacial tension to result in an optically smooth surface finish. Similarly, the choice of material for microchannel fabrication was PDMS. However, spin-coating of PS solution directly on the PDMS surface does not produce a good quality film. Therefore, a PS thin film (50-100 nm) was spin-coated on glass and then floated on water and captured on the PDMS substrate.[33] Moreover, the thermal dewetting of PS thin films on PDMS is extremely slow owing to the low surface energy of PDMS and 100 nm PS film is practically stable. So the intensified dewetting using a dewetting solution which is a mixture of solvent (MEK) non solvent (water) and a homogenizer (acetone) was adopted as reported earlier.[38] Solvent permeates in the polymer film which effectively brings down the glass transition temperature, below room temperature, and also reduces the interfacial tension making PS film unstable, while non-solvent prevents the dissolution of PS film into the solvent.[38] Earlier reported composition of dewetting mixture (water, MEK, and acetone in a volumetric ratio of 15:7:3) intensifies dewetting of PS films on hydrophilic surfaces (glass and silicon) to a great extent, and dewetting of 50 nm film completed within a few minutes. However, when the same composition of the dewetting mixture was used for PS films on PDMS substrate, it resulted in very slow dewetting kinetics as well as dewetting has not completed in most of the portion of the PS film to give well-separated spherical droplets. Therefore the water composition in the dewetting mixture was decreased to 50% (water, MEK, and acetone in a volumetric ratio of 10:7:3) to facilitate faster dewetting kinetics.[39] Once the dewetting is completed the samples were allowed to dry out first in ambient conditions and then in a vacuum oven at 180°C to remove any entrapped liquid in PDMS substrate or PS droplets. It was observed that the dewetting solution slightly swells the PDMS substrate, and it resulted in leaching out some of the uncrosslinked PDMS oligomers and other impurities which disturb the shape

of otherwise hemispherical PS droplets.[40] It can be seen in figure 2.2a that all the lenses have circular depressions on the curved surface of droplets, whereas these were not present when dewetting is carried out on a glass substrate as in Figure 2.2b. These irregularities on the droplet surface severely increase the disordered scattering of light and make them useless for optical applications. To overcome this defect, PDMS substrates were soaked in toluene at 60°C for 30 minutes and washed several times using hot toluene. Then washed PDMS substrates were used to transfer PS film over it and then dewetting was carried out in the dewetting mixture. Figure 2.2c shows that the PS droplets produced on washed PDMS surfaces have no such defects on them. Heating these lenses at 180°C for 4 hours further improves the quality of lenses by removing any entrapped liquid or air in the PS droplet as seen in Figure 2.2d.

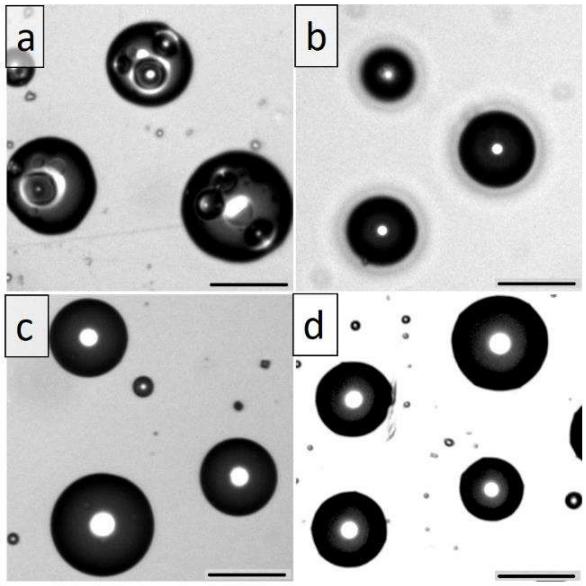

Figure 2.2 Fabrication of smooth spherical lenses of PS on PDMS surface after dewetting of PS thin film. (a) Unwashed PDMS substrate produces lenses with irregular shapes (b) PS film dewetted on a glass substrate is mostly defect-free (c) PS lenses obtained on washed PDMS substrate are defect-free (d) PS lenses on washed PDMS after thermal annealing. The scale bar is 100 µm.

However after all these processes, on very few of the lenses, some defects were visible which disturb the spherical shape of the lens. These disturbances are due to the phase separation and accumulation of impurities due to thermal annealing. The bigger dispersed appearance and scattering of light indicate that these impurities are possibly the PDMS oligomer's remnants, which remained after washing from the toluene. Some of the lenses with such disturbances are depicted in figure 2.3.

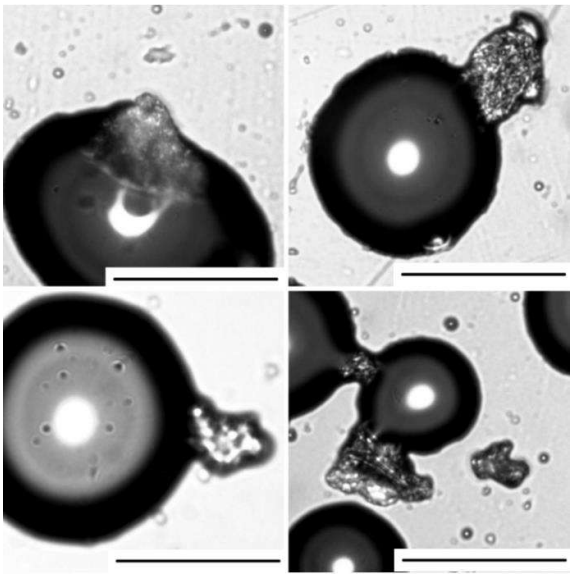

Figure 2.3 Presence of PDMS oligomers made the surface of lenses irregularly spherical, eventually, leading to the scattering of light through lenses. After heating microlenses, it was observed that PDMS oligomers were shifted on the periphery of the microlenses. However, the number of such lenses was very less. The scale bar is 50µm.

Figure 2.4 shows the SEM image of the PS microlenses fabricated on the PDMS substrate at different magnifications. Figure 2.4a shows several PS droplets whereas Figure 2.4b shows a single PS droplet at higher magnification. A small section of the PS droplet surface is further magnified in Figure 2.4c to show that the curved surface is smooth and defect free and therefore it is capable of turning into a high-quality micro-

lens. The interfacial tension between dewetting liquid and the PS and the significantly lower viscosity of PS in dewetting solution resulted in the smooth surface finish in reasonably shorter time scales. The shape of the micro-lens was examined by tilting the substrate at 80° from the horizontal position and measuring the contact angle of the lenses as shown in Figure 2.4d. Contact angles of all the lenses were found in the range of 40-70° which is significantly smaller when compared with the earlier reported PS lenses on hydrophilic substrates (glass and silicon).[16] This can be attributed to the hydrophobic nature of the PDMS substrate where dewetting liquid, which has 50% water by volume, was not able to push the contact line of the PS droplet on the PDMS substrate further. Variation in contact angle was observed with variation in droplet size. Smaller size droplets were having high contact angles than bigger droplets. Observation is compliant with the previous theoretical understanding, as the shape of the droplets is directly proportional to the radius of curvature at the top of the drop.[41]

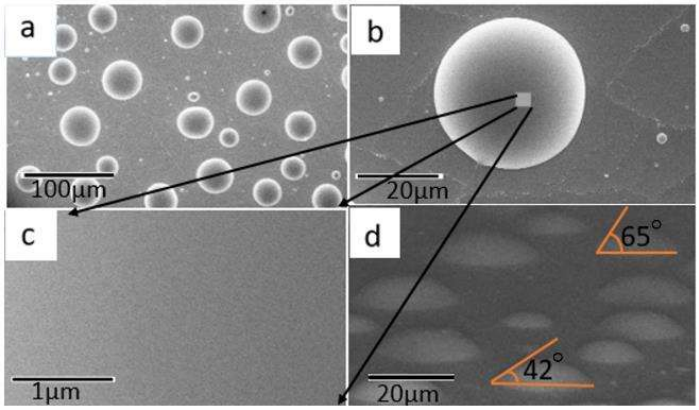

Figure 2.4 SEM image of PS droplets made on crosslinked PDMS substrate at different magnification: (a) Low magnification image showing multiple PS droplets, (b) Higher magnification image showing single PS droplet, (c) Further magnification on the droplet surface show smooth defect-free surface, (d) Tilted view shows the shape of lenses where contact angle is found in the range of 40-70°.

2.4.2 Magnification and Resolution of Microlenses

To examine the magnifying capability of the fabricated micro-lenses, these were kept inverted over a commercially available compact disk (CD), which has 780 nm wide channels (1.5 μm pitch) and observed through a 20X (N.A. 0.4) objective lenses in an upright optical microscope, as shown in the schematic diagram Figure 2.5aIt can be seen in the subsequent image sections Figure 2.5b and 2.5c that micro-lenses of different size provide high magnification without significant spherical aberration. The amount of additional magnification achieved was nearly five times over the microscope magnification depending on the lens size, shape, and position of the objective lens. This add-on magnification can be further increased by reducing the size of micro-lenses as well as placing objects closer to the focal points of the micro-lenses.

Micro-lenses have also enabled the microscope to resolve CD patterns with a lower magnification 10X (N. A. 0.25) objective, however with a noticeable spherical aberration as seen in Figure 2.5d. Without microlenses, CD patterns were not visible from the same 10X objective, which shows that these lenses can significantly improve the resolution of the given microscope. This enables using ordinary, inexpensive microscopes for high-resolution imaging without the need for expensive state-of-the-art objective lenses. In the earlier reported work, Yang et al[36] have demonstrated a similar application of PMMA lenses however using a significantly complicated process. In comparison, this work shows good magnification and the micro-lenses are significantly easier to fabricate and use, with high magnification and depth of field.

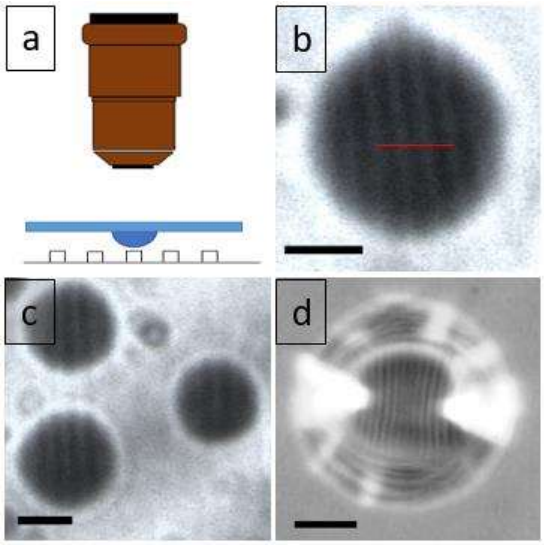

Figure 2.5 Different sizes of lenses showed different magnification and image quality in terms of contrast and brightness. a) Schematic diagram of imaging setup. b) and c) image of the CD pattern under the micro-lens in the size range 30-50 µm with 20X objective. d) Image of CD pattern with a 10X objective lens. The scale bar is 20µm (for portions outside the micro-lens) and 4.5µm (for portions inside the microlens).

By changing the position of the objective lens, an inversion of the image is observed. In Figure 2.6 Images of the CD pattern show that using microlenses, the depth of focus is 10 to 15 times more than without microlenses. Images from a to i are captured at each 20µm movement of the microscope objective in the z-direction, using a 20X/(NA 0.40) objective. For the first 60 micrometers Images are erected and tend to focus on a point. In the fourth Image a point focus is observed and subsequently moving the objective lens, an inverted image is developed which finally gets blurred after 60-80 micrometer movement of the objective lens. Effectively up to 100 micrometers of depth is visible under the combination of objective lenses and microlenses. Meanwhile, there is a point where the CD pattern is visible through the objective lens as well as a microlens, see figure 2.6f. When a section of figure 6f is magnified we can see the CD pattern without

(Outside) microlens, as shown separately. In properly magnified Images (a,h,i) Compared with the scale bar shows that the pattern inside the lens is almost 10 times more magnified than outside the lens.

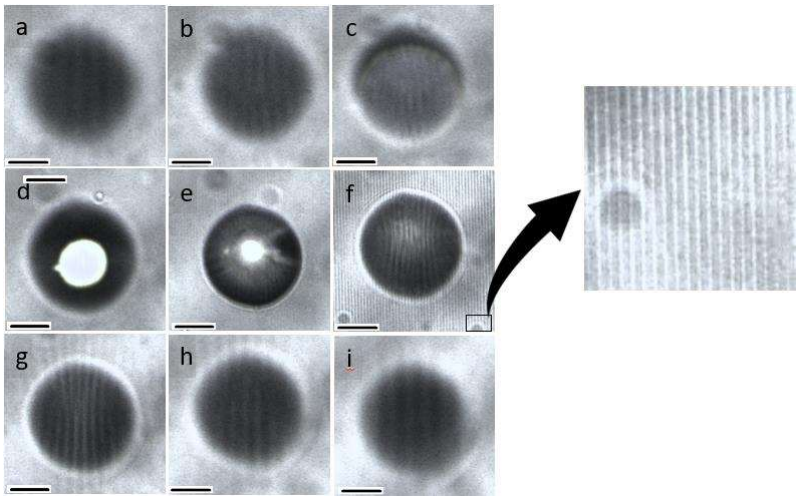

Figure 2.6 Subsequent Images of a particular microlens focused on the CD pattern after 20 micrometer movement of the Objective lens in the Z direction. CD pattern can be seen with a robust focus. The depth of field is much higher with a combination of microlenses and objective lenses when compared to the depth of field with an objective lens alone. The scale bar is 50µm

Moreover, It is also observed that the magnification property of the lenses is not limited to the spherical lenses only. Figure 2.7 shows that a significant amount of magnification was observed through the lenses that are not perfectly spherical and have rather an irregular shape. This property makes us rather comfortable to consider worries about the sphericity of the lenses. Even if due to irregularities in the surface of the substrate or other impurities interaction, if microlenses are a bit distorted, it would not hamper the imaging process.

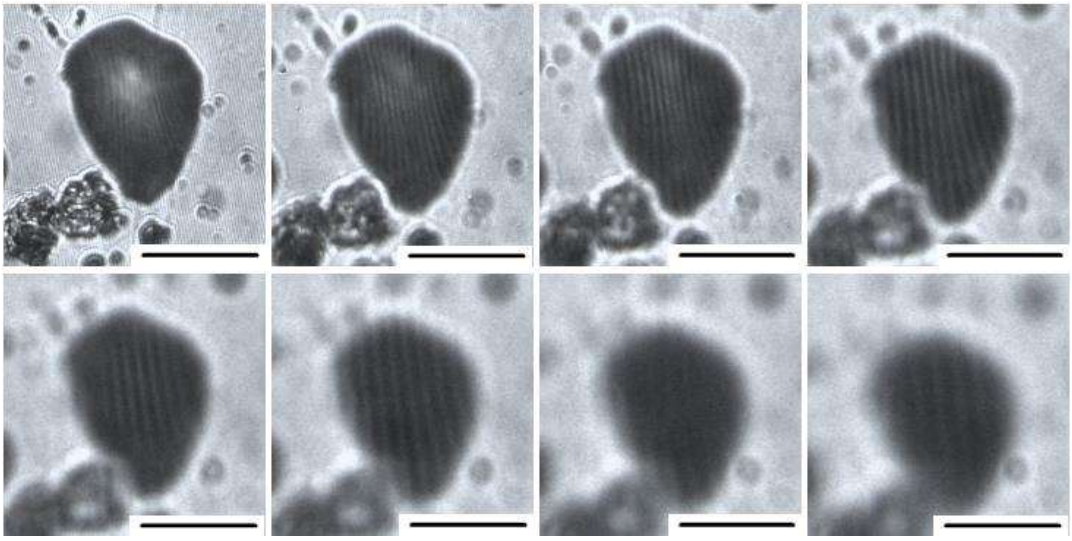

Figure 2.7 Irregular shape lenses focused on a CD pattern showing magnification and resolution of CD pattern. Irregular shape lenses did not pose a problem in imaging and provided significant magnification with a robust depth of focus. The scale bar is 50µm.

Next, to examine micro-lens performance in visualizing moving latex particles inside the microchannel, inverted lenses with the curved surface facing downward were placed on the microchannel of depth 100µm. Bonding between the bottom section of PDMS with microchannel and top cover having PDMS substrate with microlenses was done by using a thin uncrosslinked PDMS layer as a glue between them as shown in Experimental Section. Suspended PS particles of 3.0 µm size with a number density of 7×10^9 particles/ml (~10% w/w) were diluted to different concentrations and flown inside the microchannel and observed using a 20X objective lens. Particle suspensions were found to be well dispersed and stable during the time of the observation. Figure 2.8a shows well-dispersed particles inside the channel with no visible agglomeration. Particles were found to be better resolved under the micro-lenses. However, the contrast of the image is slightly

poorer due to the movement of particles as well as an aqueous medium instead of air (Figure 2.8b–d).

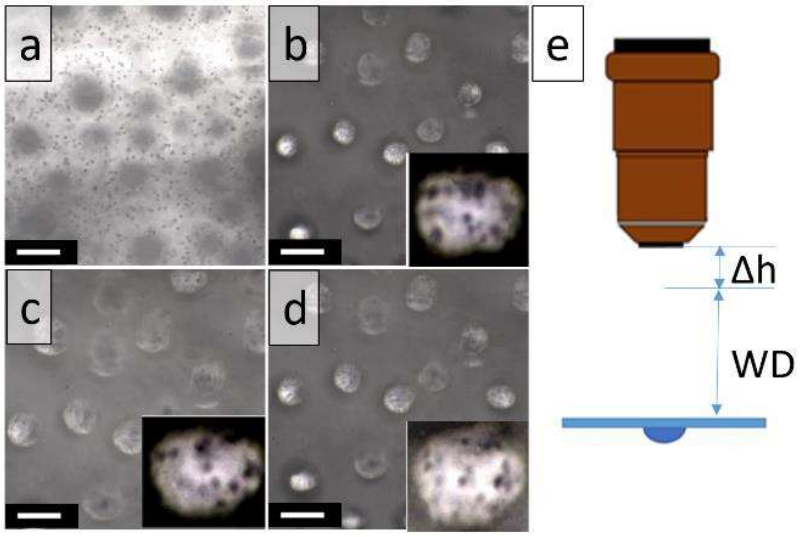

Figure 2.8 Images of flowing PS particles at different depths of focus. (a) Direct focusing on particles in the channel shows that particles are uniformly distributed; (b), (c), and (d) are the images obtained when focusing on particles with increasing depth of focus in the microchannel as the microscope objective is moved downwards by 30, 60, and 90 µm after focusing at the micro-lens. e) Schematic diagram showing the arrangement of the microscope objective, the working distance (WD), and the downward displacement (Δh). The scale bar is 20 µm.

2.4.3 Quantification of Observed Particles

As we move, the microscope objective downwards (Figure 2.8e) different particles flowing at different depths of the microchannel get focused however this also depends on the number of particles present under a microlens as discussed in the next section. If there are very few particles then almost all of them are distinguishable at every depth of focus, whereas if there are too many particles then the out-of-focus particles cannot be properly resolved as separate particles. This is more evident from Figure 2.9 which shows average

number of particles visible through microlens plotted against the actual number of particles present under the same micro-lens assuming a uniform distribution of particles in the suspension. For this, we have calculated the actual number of particles flowing at any instance under a microlens of known diameter by calculating the volume of suspension lying just below the microlens and multiplying it with the number density of particles. Particle suspensions of number density varying over two orders in the range of 7×10^6 to 7×10^8 particles/ml were flown in the microchannel and examined using an optical microscope in conjunction with PS microlenses. In Figure 2.9 blue dotted line represents an ideal case when all the particles lying under the microlens are visible. However, we observe a greater departure from this line for a higher concentration of particles. This can be attributed to the fact as there is a crowding of particles under the lens, only particles that are in good focus are distinguishable, and therefore increasing degrees of undercounting of particles occur at higher concentrations of particles. However, this can be corrected by selecting a shallower microchannel where lesser particles occupy the volume under the microlens for the same number of particles per unit volume. Whereas, at lower concentrations where almost all the particles lying under the microlens are visible and distinguishable even if they are slightly away from the focus. Since, at a lower concentration, there were lenses under which no particles were present, we considered the lenses only where a particle is visible. Thus, we observed over counting of particles because of the practical reasons for imaging in the optical microscope. When we do not see any particle under a lens it is not possible to focus and hence in averaging out the number of particles under a microlens, lenses without any particles are undercounted.

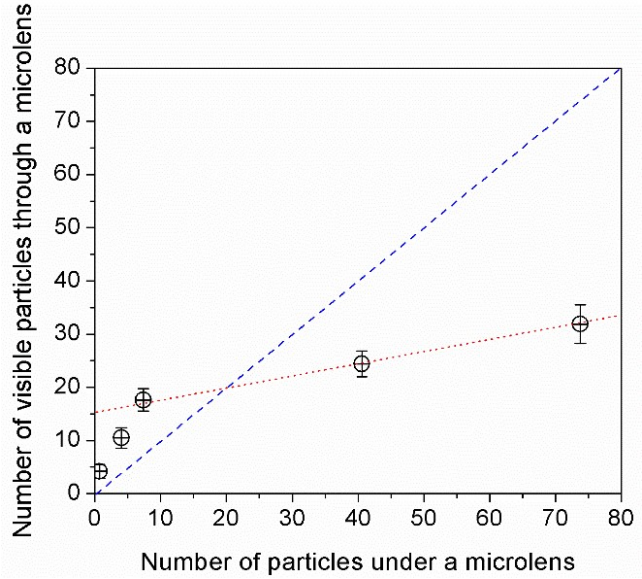

Figure 2.9 Average number of particles visible through one micro-lens of diameter 34-38 μm plotted against the actual number of particles present under the same micro-lens assuming a uniform distribution of particles in the suspension. The Blue dotted line represents the case when all the particles are visible through the microlens.

2.4.3.1 *Calculation method for particle density estimation*

Nonetheless, the trend depicted in figure 2.9 is sufficient to provide us with a tool to estimate the number of particles in an unknown suspension with very good accuracy (greater than 90%) when the particle concentration in the suspension is in the range of 10^8 to 10^9 particles/ml by interpolation on the observed dotted red line in Figure 9. Even at lower concentrations of particles, we can reduce overcounting by fixing the position of the objective lens and taking into account the contribution of the lenses with no particle present. A sample calculation is shown here for the particle density estimation.

Volume Under the lens

The average diameter of lenses observed = 36.639 μm

Average area of the lenses = 1053.78 μm^2

Since the depth of the channel is 100μm, Average volume occupied under the lens area = 1053.78×100 μm^3

= 1.05378 × 10^{-7} cm^3

The concentration of Polystyrene particles in the flowing solution

Original concentration of the particles in the suspension = 7 × 10^9Particles/ml

After diluting the suspension 10 times concentration of particles in the suspension = 7 × 10^8 Particles/ml

Using the formula $\mathbf{C_iV_i = C_fV_f}$ Suspension is diluted into four different concentrations as 7 × 10^8, 3.85 × 10^8, 7 × 10^7, 3.85 × 10^7 and 7 × 10^6 Particles/ml (Ci is the initial particle concentration and Vi is the initial volume of the suspension and Cf is Final particle concentration and Vf is the final volume of the suspension)

Now,

Concentration of the particles under the lens volume = Concentration of particles/cm^3 × Average volume occupied under the lens.

No. of particles present under the lens volume is calculated to be 73.77, 40.57, 7.37, 4.05, 0.73 for a concentration range of 7 × 10^8, 3.85 × 10^8, 7 × 10^7, 3.85 × 10^7 and 7 × 10^6 Particles/ml respectively.

Estimation of the number of particles in a given sample using the graph provided in figure 2.9-

For high particle concentration in the suspension, the relation between the observed number of particles and the actual number of particles is established (Depicted by the red line in figure 2.9)

$Y = 0.213P + 16$

Where Y is the number of visible particles through a lens, and x is the theoretically calculated average number of particles under the lens, which gives

$$P = \frac{Y-16}{0.213}$$

Since this value of X is the theoretical number of particles in the volume covered under the lens, the actual number of particles in the suspension can be calculated as

Particles per milliliter = P/Volume under the lens (cm^3)

= P/ Area of the lens cm^2 x depth of channel (cm)

= 10^4 x P/Area of lens cm^2 (Considering the depth of channel as 100μm)

2.4.4 Experimental Observation and Future Scope

During all the experiments it was observed that micro-lenses were firmly placed on the PDMS surface and we have not noticed any instance of lens detachment under typical flow conditions. Micro-lens embedded system was used repeatedly at least for 10 hours with minimal deterioration in the image quality. However, after several experiments, we have noticed poor quality images possibly due to cross-contamination of buffer/surfactants present in the particle suspension onto the microlens which had roughened the lens surface and thus increased the random scattering of light. In homogeneous dewetting, all the droplets (microlenses) have different sizes and hence

different focal lengths. We observed that the microlenses in the size range of 25-55 µm are best suited for simultaneous focusing through all the lenses. Using this technique, a simple microscope can be used for high-resolution imaging in various applications to analyze biological assays. For counting a particular type of cell, tissue, bacteria, or other biological entities we can use this technique, which can give a good number estimate without counting these entities sequentially as in a flow cytometer. This can immensely increase the throughput and simultaneously reduce the cost of counting. Using faster image processing techniques and increasing the number of lenses in the channel we can further improve the resolution and throughput.

2.5 CONCLUSION

The present study shows that the microlenses obtained by dewetting of PS thin-film on PDMS substrate can effectively focus on the moving particles in the microfluidic channel. These lenses significantly increase the magnification and contrast of the image by collecting more diffracted light from the object. We have reported a clearly resolved images of 780 nm features on a stationary object and 3 µm suspended particles in an aqueous medium moving inside a microfluidic channel using these lenses in conjunction with a standard optical microscope. This shows a very promising application to observe various biological analytes like bacteria, viruses, platelets, red blood cells, and other microorganisms which are either not visible or barely distinguishable under a standard pathology lab microscope. This also opens up the application of microlens-incorporated microfluidic chips to be used as disposable flow cytometers. Moreover, it requires a very small volume of sample to estimate the particles or analytes. Since it uses commodity polymers like PS and PDMS these chips are inexpensive and do not add any significant cost to the already available pathology lab infrastructure. Furthermore, since moving

particles can be effectively tracked, the applications such as particle velocimetry can also be developed using this technique. This technique can also be extended to a mobile pathology lab by using a cell phone camera instead of an optical microscope for observing and counting objects as small as 10 μm.

2.6 REFERENCES

[1]. Li, L.; Yi, A. Y. Microfabrication on a Curved Surface Using 3D Microlens Array Projection. J. Michromech. Microeng. 2009, 19, 1-9.

[2]. Wu, M.; Whitesides, G. M. Fabrication of Two-Dimensional Arrays of Microlenses and Their Applications in Photolithography. J Michromech Microeng. 2002, 12, 747–758.

[3]. Kawai, S. Free-Space Multistage Optical Interconnection Networks Using Micro Lens Arrays. J. Light. Technol. 1991, 9, 1774–1779.

[4]. Edwards, C. A.; Presby, H. M.; Dragone, C. Ideal Microlenses for Laser to Fiber Coupling. J. Light. Technol. 1993, 11, 252–257.

[5]. Zhou, X.; Peng, Y.; Peng, R.; Zeng, X.; Zhang, Y.; Guo, T. Fabrication of Large-Scale Microlens Arrays Based on Screen Printing for Integral Imaging 3D Display. ACS Appl. Mater. Interface 2016, 36, 24248-24255.

[6]. Möller, S.; Forrest, S. R. Improved Light Out-Coupling in Organic Light Emitting Diodes Employing Ordered Microlens Arrays. J. Appl. Phys. 2002, 91, 3324–3327.

[7]. Qu, Y.; Kim, J.; Coburn, C.; Forrest, S. R. Efficient, Nonintrusive Outcoupling in Organic Light Emitting Devices Using Embedded Microlens Arrays. ACS Photonics 2018, 5, 2453–2458.

[8]. Stoklasa, B.; Motka, L.; Rehacek, J.; Hradil, Z.; Sa, L. L. Wavefront Sensing Reveals Optical Coherence. Nat. Commun. 2014, 5, 1–7.

[9]. Nussbaum, Ph.; Volkel, R.; Herzig, H. P.; Eisner, M.; Haselbeck, S. Design, Fabrication and Testing of Microlens Arrays for Sensors and Microsystems. Pure Appl. Opt. 1997, 6, 617-636.

[10]. Wang, W.; Fang, J.Variable Focusing Microlens Chip for Potential Sensing Applications. IEEE Sens. J. 2007, 7, 11-17.

[11]. Sinigirev, A.; Kohn, V.; Sinigireva, I.; Lengeler, B. A Compound Refractive Lens For Focusing High-Energy X-Rays. Nature 1996, 384, 49-51.

[12]. Ruffieux, P.; Scharf, T.; Philipoussis, I.; Herzig, H. P.; Voelkel, R.; Weible, K. J. Two Step Process for the Fabrication of Diffraction Limited Concave Microlens Arrays. Opt. Express 2008, 16, 19541–19549.

[13]. Schena, M.; Shalon, D.; Davis, R. W.; Brown, P. O. Quantitative Monitoring of Gene Expression Patterns with a Complementary DNA Microarray. Science 1995, 270, 467-470.

[14]. Liu, J.; Chang, M.; Ai, Y.; Zhang, H.; Chen, Y. Fabrication of Microlens Arrays by Localized Hydrolysis in Water Droplet Microreactors. ACS Appl. Mater. Interface 2013, 5, 2214-2219.

[15]. Becker, H.; Heim, U. Hot Embossing as a Method for the Fabrication of Polymer High Aspect Ratio Structures. Sens. Actuator A Phys. 2000, 83, 130–135.

[16]. Verma, A.; Sharma, A. Enhanced Self-Organized Dewetting of Ultrathin Polymer Films under Water-Organic Solutions: Fabrication of Sub-Micrometer Spherical Lens Arrays. Adv. Mater. 2010, 22, 5306–5309.

[17]. Lee, J. Y.; Hong, B. H.; Kim, W. Y.; Min, S. K.; Kim, Y.; Jouravlev, M. V.; Bose, R.; Kim, K. S.; Hwang, I.-C.; Kaufman, L. J.; Wong, C. W.; Kim, P.; Kim, K. S. Near-field focusing and magnification through self-assembled nanoscale spherical lenses Nature 2009, 460, 498–501.

[18]. Jin, Y.; Hassan, A.; Jiang, Y. Freeform Microlens Array Homogenizer for Excimer Laser Beam Shaping. Opt. Express 2016, 24, 2467–2475.

[19]. Ro, K. W.; Lim, K.; Shim, B. C.; Hahn, J. H. Integrated Light Collimating System for Extended Optical-Path-Length Absorbance Detection in Microchip-Based Capillary Electrophoresis. Anal. Chem. 2005, 77, 5160–5166.

[20]. Song, Y. M.; Xie, Y.; Malyarchuk, V.; Xiao, J.; Jung, I.; Choi, K.; Liu, Z.; Park, H.; Lu, C.; Kim, R.; Li, R.; Crozier, K. B.; Huang, Y.; Rogers, J. A. Digital Cameras with Designs Inspired by the Arthropod Eye. Nature 2013, 497, 95–99.

[21]. Duparré, J. W.; Wippermann, F. C. Micro-Optical Artificial Compound Eyes. Bioinspir. Biomim. 2006, 1, 1–16

[22]. Shogenji, R.; Kitamura, Y.; Yamada, K.; Miyatake, S.; Tanida, J. Bimodal Fingerprint Capturing System Based on Compound-Eye Imaging Module. Appl. Opt. 2004, 43, 1355–1359.

[23]. Chan, E. P.; Crosby, A. J. Fabricating Microlens Arrays by Surface Wrinkling. Adv. Mater. 2006, 18, 3238–3242.

[24]. Li, L.; Yi, A. Y. Development of a 3D Artificial Compound Eye. Opt. Express 2010, 18, 18125–18137.

[25]. Florian, C.; Piazza, S.; Diaspro, A.; Serra, P. Direct Laser Printing of Tailored Polymeric Microlenses. ACS Appl. Mater. Interface 2016, 8, 6–10.

[26]. Zhang, D.; Xu, Q.; Fang, C.; Wang, K.; Wang, X.; Zhuang, S.; Dai, B. Fabrication of a Microlens Array with Controlled Curvature by Thermally Curving Photosensitive Gel Film beneath Microholes. ACS Appl. Mater. Interface 2017, 19, 16604–16609.

[27]. Jung, H.; Jeong, K. Monolithic Polymer Microlens Arrays with High Numerical Aperture and High Packing Density. ACS Appl. Mater. Interface 2015, 7, 2160–2165.

[28]. Li, X.; Tian, H.; Ding, Y.; Shao, J.; Wei, Y. Electrically Templated Dewetting of a UV-Curable Prepolymer Film for the Fabrication of a Concave Microlens Array with Well-De Fi Ned Curvature. ACS Appl. Mater. Interface 2013, 5, 9975–9982.

[29]. Yong, J.; Chen, F.; Yang, Q.; Du, G.; Bian, H.; Zhang, D.; Si, J.; Yun, F. Rapid Fabrication of Large-Area Concave Microlens Arrays on PDMS by a Femtosecond Laser. ACS Appl. Mater. Interface 2013, 5, 9382–9385.

[30]. Reiter, G. Dewetting of Thin Polymer Films. Phys. Rev. Lett. 1992, 68, 75-78.

[31]. Sharma, A.; Reiter, G. Instability of Thin Polymer Films on Coated Substrates: Rupture Dewetting and Drop Formation. J. Colloid Interface Sci. 1996, 178, 383-399.

[32]. Kargupta, K.; Sharma, A. Creation of Ordered Patterns by Dewetting of Thin Films on Homogenous and Heterogenous Substrates. J. Collod Interface Sci. 2002, 245, 99-115.

[33]. Mukherjee, R.; Bandyopadhyay, D.; Sharma, A. Control of Morphology in Pattern Directed Dewetting of Thin Polymer Films. Soft Matter 2008, 4, 2086-2097.

[34]. Kim, J.; Nayak, S.; Lyon, L. A. Bioresponsive Hydrogel Microlenses. J. Am. Chem. Soc. 2005, 127, 9588–9592.

[35]. Ellison, J. C.; Mundra, K. M.; Torkelson, M. J. Impact of Polystryrene Molecular Weight and Modification to The Repeat Unit Structure on The Glass Transition-Nanoconfinement Effect and Cooperativity length Scale. Macromolecules, 2005, 38, 1767-1778.

[36]. Yang, Y.; Huang, X.; Zhang, X.; Jiang, F.; Zhang, X.; Wang, Y. Supercritical Fluid-Driven Polymer Phase Separation for Microlens with Tunable Dimension and Curvature. ACS Appl. Mater. Interface 2016, 8, 8849-8858.

[37]. Verma, A.; Sekhar, S.; Sachan, P.; Reddy, P. D. S.; Sharma, A. Control of Morphologies and Length Scales in Intensified Dewetting of Electron Beam Modified Polymer Thin Films under a Liquid Solvent Mixture. Macromolecules 2015, 48, 3318-3326.

[38]. Verma, A.; Sharma, A. Submicrometer Pattern Fabrication by Intensification of Instability in Ultrathin Polymer Films under a Water-Solvent Mix. Macromolecules 2011, 44, 4928-4935.

[39]. Yadav, P.; Verma, A. Intensified Dewetting of Polystyrene Thin Film Under Water-Solvent Mixture: Role of Solvent Composition. Bull. Mater. Sci. 2020, 43, 170

[40]. Lee, J. N.; Park, C.; Whitesides, G. M. Solvent Compatibility of Poly(Dimethylsiloxane) Based Microfluidic Devices. Anal. Chem. 2003, 75, 6544–6554.

[41]. Shull, K. R.; Karis, T. E. Dewetting Dynamics for Large Equilibrium Contact Angles. Langmuir, 1994, 10, 334-339.